The Egyptian Journal of Radiology and Nuclear Medicine (2014) **45**, 849–858

Egyptian Society of Radiology and Nuclear Medicine

The Egyptian Journal of Radiology and Nuclear Medicine

www.elsevier.com/locate/ejrnm
www.sciencedirect.com

ORIGINAL ARTICLE

Diagnostic yield of combined magnetic resonance spectroscopy and diffusion weighted imaging in intracranial neoplasms

Ayat E. El Sherbeny [a,*], Mohamad H. El-Shafey [a], Sheref L. Biomy [b], Ahmad A. Shakal [c], Mohamad M. Hefeda [a], Abdel-Hamid R. Seiam [d]

[a] *Radiodaignosis Department, Faculty of Medicine, Tanta University, Egypt*
[b] *Pathology Department, Faculty of Medicine, Tanta University, Egypt*
[c] *Neurosurgery Department, Faculty of Medicine, Tanta University, Egypt*
[d] *Neurology Department, Faculty of Medicine, Al-Azhar University, Egypt*

Received 2 January 2014; accepted 2 May 2014
Available online 27 May 2014

KEYWORDS

Brain;
Neoplasm;
MRS;
MRI;
DWI

Abstract *Purpose:* Our intention was to evaluate the role of combined diffusion magnetic resonance imaging and spectroscopy in diagnosis and grading of brain tumors.
Materials and methods: Ninety-three included cases underwent magnetic resonance imaging (MRI) and magnetic resonance spectroscopy (MRS) of the brain lesion, stereotactic or open biopsies and histopathological examination. MRI protocol included DWI and calculated ADC values. Multivoxel MRS spectroscopic technique (MVS) was used and all MRS metabolic parameters were obtained.
Results: High grade tumors had significantly lower ADC values than low grade tumors ($P < 0.001$). ADC values were the lowest in lymphoma (0.54×10^{-3} mm^2/s) and the highest in craniopharyngioma (1.9×10^{-3} mm^2/s). MRS revealed a statistically significant difference in CHO/NAA and CHO/Cr ratios between low and high grade tumors with $P < 0.01$ and $P < 0.001$, respectively. The mI/Cr ratio and presence of lactate, lipid and taurine also aided in differentiation and grading of brain tumors. The overall MRI/MRS sensitivity and specificity were 91%, 90.5%, respectively.
Conclusion: MRS has a robust diagnostic accuracy in cases of well defined high or low grade brain neoplasms. ADC value had the ability to confirm and differentiate low from high grade tumors in many situations where there were diagnostic confusions with MRS due to borderline values.

1. Introduction

Brain tumors represent an important cause of morbidity and mortality and are frequently difficult to treat. Grading of intracranial neoplasm is of prognostic role and has an important inference in further management decision. Clearly, the main

* Corresponding author. Tel.: +20 1005546903.
E-mail address: Ayat.Ibraheem@yahoo.com (A.E. El Sherbeny).
Peer review under responsibility of Egyptian Society of Radiology and Nuclear Medicine.

0378-603X http://dx.doi.org/10.1016/j.ejrnm.2014.05.001

purpose of progressive development of non invasive imaging techniques, like MRI/MRS techniques, is to improve diagnostic accuracy and minimize the need to more invasive diagnostic options. For tumors where surgical resection is not the initial therapeutic option, an accurate non-invasive diagnosis would avoid an invasive procedure (1). Evolution in MRI procedures has improved its value for assessing brain tumors both before and after treatment. DWI is one of the most widely available, practical, and robust techniques (2). It reveals the Brownian motion of tissue water. The apparent diffusion coefficient (ADC) is principally determined by tissue cellularity, as measured by the intracellular and extracellular volume fractions (3). ADC is a helpful maneuver in discrimination between certain types of brain tumors, like malignant lymphomas versus glioblastomas and metastatic tumors, and ependymomas versus PNETs (4). MRS contributes to metabolic assessment of brain tumors outside that can be obtained from anatomic imaging. Brain metabolites assessed by MRS can characterize features of neuronal integrity (NAA), cell membrane proliferation or degradation (Cho), energy metabolism (Cr) and necrotic transformation of brain or tumor tissue (lipid/lactate) (5). The field of clinical applications of proton MRS (1H MRS) in brain neoplasms is broad and includes; classification and grading of tumor type (6), detect subtle differences between low grade brain tumors (7), differentiating brain abscesses from cystic or necrotic tumors, evaluating the response of brain tumors to different therapeutic options and ability to differentiate between tumor recurrence and radiation necrosis (8).

2. Materials and methods

One hundred and forty-five consecutive cases were recruited. All patients underwent proper history taking, MRI and MRS of the brain lesion, stereotactic or open biopsy and histopathological examination of the tumor as a gold standard method to provide accurate diagnosis.

2.1. MRI protocol

MRI 1.5-Tesla unit was used for all patients at the radiodiagnosis department at Tanta University. Scan parameters used were; T1 weighted images (T1 WI) with short TR 400–500 ms. and short TE 15–25 ms. T2 weighted spin echo images (T2 WI) with long TR 3500–5000 ms and long TE 80–100 ms, Fluid Attenuation Inversion Recovery (FLAIR) images with TR 2000–3000 ms. TE 15–25 ms, inversion time TI 700 ms and gadolinium enhanced T1 images. In addition, diffusion weighted images (DWI) were obtained by using an axial echo – planar SE sequence (6000/92 s) [TR/TE], one average, 5 mm section thickness. DW images and ADC maps were acquired by using b values of 0, 500 and 1000 s/mm^2 applied in the X, Y and Z directions. Tumoral core and peri-tumoral high signal intensity areas were sampled manually, while preferably avoiding cystic and necrotic areas. Standard mean ADC values were calculated automatically and expressed in 10–3 mm^2/s. In all cases, normal, tumoral and peritumoral regions were defined on the bases of the following imaging features: (1) Normal tissue; an area containing no enhancement and normal signal intensity on T2 WIs and)FLAIR(, (2) Tumoral area; a region containing a well-defined solid portion, contrast enhancement or abnormal signal intensity on T2 WIs and (FLAIR), (3) Peritumoral area, a region containing no enhancement and shows high signal intensity on T2 WIs and (FLAIR) and peri-lesional edema.

2.2. MRS protocol

All cases were evaluated by multivoxel spectroscopic technique (MVS). In MVS, we applied 16×16 grid avoiding areas that show hemorrhage or necrosis and avoiding contamination from nearby bone or CSF spaces. From this grid only 9 or 8 separate voxels (voxel size, $15 \times 15 \times 10$ mm) were individually placed in the area of the tumor, peritumoral area and contralateral normal brain area. We used point resolved spectroscopy (PRESS) with parameters TR/TE 1000/144 and 1500/35. Both long and short TE (144 and 35 ms) were used. Long TE was used to visualize peak intensity of CHO, Cr, Mi and NAA, to obtain CHO/NAA CHO/Cr and mI/Cr ratios and to determine the presence of Lactate (Lac). Short TE was mainly used to illustrate Lipid (Lip) peak. In addition, alanine and taurine levels were obtained from intralesional parts.

2.3. Biopsy and histopathology methods

Open or stereotactic biopsies were obtained by an expert neurosurgeon. In our study histopathology was done for all cases except in 8 cases of metastasis and one case of lymphoma which were unfit for surgical procedure with a known history of primary tumor. Thirty-eight cases underwent open biopsy and 46 cases underwent stereotactic biopsy. Formalin-fixed paraffin-embedded tissue sections were used. The sections were then evaluated for the presence of nuclear pleomorphism, mitotic figures, micro vascular proliferation, and necrosis. Grading and typing of tumors was based on the World Health Organization (WHO) criteria. According to WHO, tumors were classified into low grade tumors (I–II) and high grade tumors (III–IV).

2.4. Data analysis

Statistical data analysis was performed, using statistical package for social science (SPSS), version 16. For interpretation of results, P value of $\leqslant 0.05$ was considered significant.

3. Results

The 93 patients who proved histopathologically to have brain tumors, included 51 males (55%), 42 females (45%) with their ages ranging from 10 to 73 years. The most common age of incidence of brain tumor in our patients was >50 years (40.8%).

3.1. According to histopathological findings

The primary tumor of origin represented 84%, while metastatic brain tumors in 16% cases. Out of 93 included patients, 34 (31%) cases had low grade tumors (Grades I, II), while 64 cases (69%) had high grade tumors (Grades III and IV). Sixty (64.5%) cases were glial tumor in origin, while 33 cases (35.5%) were non glial tumor in origin. Glioblastoma

multiformis was the most common of glial tumors (49.2% of glial tumors), while metastasis was the most common of non glial tumors (45.4%). According to WHO classification (9), low grade tumors are grades I, II and high grade tumors are grades III and IV, (Table 1).

3.2. According to MRI findings

Intra axial tumors represented 82 cases (88.2%) while extra axial tumors were 11 (11.2%) cases. The most common intra axial tumor in our patients was glioblastoma multiformis (GBM) (32% of all intra axial tumors), while the most common extra axial tumor was meningioma (45.4% of all extra axial tumors). The diagnosis is based on signal intensity, heterogenousity, necrosis, hemorrhage, edema and mass effect, (Table 1). The DWI calculated ADC values from tumoral areas were the lowest in lymphoma ($0.54 + 0.18 \times 10^{-3}$ mm^2/s) and the highest in craniopharyngioma (1.9×10^{-3} mm^2/s). There was highly statistically difference between high and low grade tumors regarding the calculated ADC values (P value < 0.001). High grade malignant tumors had significantly lower ADC values than those of low grade tumors, (Fig. 1). No significant difference was recorded between ADC values of different types of tumor of the same grade.

3.2.1. According to MRS findings

The calculated CHO/NAA and CHO/Cr ratios showed significant difference between low and high grade tumors with no significant difference between different tumors of the same grade, (Fig. 2). There was significant difference in CHO/NAA mean values between low and high grade tumors with P value (< 0.01).

Similarly, there was highly significant difference in CHO/Cr mean values between low and high grade tumors with P value (< 0.001) (Fig. 2). Myoinositol which is considered as a glial marker also added additional diagnostic value to MRS. Our findings showed that Myoinositol was higher in patients with low grade glioma and lower in those who had high grade glioma. Calculated mI/Cr ratio was higher in patients with low-grade astrocytoma, ependymoma, oligodendroglioma and lower in patients with anaplastic astrocytoma, choroid plexus carcinoma and GBM, (Fig. 3).

The presence of lipids and lactate was also aided in grading of brain tumors. Both long and short TE (144 and 35 ms) respectively were used to evaluate the presence of lactate and lipid. The lactate peak was well demonstrated on long TE while the lip peak was much more evident on short TE. Low grade gliomas showed absent or low lactate and lipid. With increasing malignancy, there was an increase in lactate and lipid peaks with a significant difference for lipid between low and high grade tumors (Fig. 4). All the cases of GBM, medulloblastoma, germinoma, lymphoma, choroid plexus carcinoma and metastases show high lipid/lactate peaks. Craniopharyngioma is a benign tumor that showed high lipid lactate due to its cholesterol content (fig. 5).

In the present study, additional MRS diagnostic value was also found in the differentiation between primary high grade brain tumors (GBM and lymphoma) and metastatic tumors using the calculated CHO/NAA and CHO/Cr ratios from perilesional voxels. The primary tumors showed increased ratios (more than 1.2) which denote peri-lesional infiltration, while metastatic tumors showed normal ratios denoting peri-lesional edema. Moreover, MRS showed a significant role in differentiation between medulloblastoma and ependymoma by the presence of taurine (at 3.4 ppm) which is a specific metabolite for medulloblastoma (Table 2).

MRS has also aided in the differentiation between pituitary adenoma and craniopharyngioma, as pituitary adenoma showed high choline while craniopharyngioma showed high lipid, lactate (cholesterol content) with absence of other metabolites. In the present study MRS showed the ability to confirm the diagnosis of Meningioma cases by the presence of alanine (at 1.4 ppm) which is a specific metabolite for meningioma. MRS was insignificant in differentiation between meningioma and acoustic neuroma because both tumors have same spectroscopic pictures (Table 3).

MRS shows ability to differentiate between tumor recurrence and radiation necrosis, tumor recurrence showed high Cho/Cr ratio, and Cho/NAA, while radiation necrosis showed high lipid/lactate levels with normal ratios of Cho/Cr ratio, and Cho/NAA. The overall diagnostic accuracy of combined MRI/MRS in 93 cases in whom histopathology were obtained was 91% with considerable high sensitivity (91%) and specificity (90.5%) (Figs. 6–8).

In few cases MRS was not able to accurately diagnose the brain tumor type or grade. One case of gliomatosis cerebri was initially diagnosed as low grade glioma, 2 cases of astrocytoma grade II were diagnosed as anaplastic astrocytoma, 2 cases of anaplastic astrocytoma were diagnosed as GBM, one case of ependymoma was diagnosed as low grade astrocytoma and 2 cases of glioblastoma multiformis were diagnosed as

Table 1 Classification of brain tumors of included 93 cases according to WHO classification (9).

High grade tumors	*N* (%)	Low grade tumors	*N* (%)
1:GBM	32 (34.4)	1:Low grade astrocytoma (II)	16 (17.2)
2:Metastases	15 (16.1)	4:Meningioma	5 (5.4)
3:Anaplastic astrocytoma	5 (5.4)	2:Oligodendroglioma	2 (2.2)
4:Lymphoma	4 (4.3)	3:Ependymoma	2 (2.2)
5:Medulloblastoma	3 (3.2)	6:Pituitary adenoma	2 (2.2)
6:Gliomatosis cerebri	2 (2.2)	5: Acoustic neuroma	1(1.1)
7:Germinoma	2 (2.2)	7:Craniopharyngioma	1(1.1)
8:Choroid plexus carcinoma	1 (1.1)	–	
Total	64 (69%)	Total	29 (31%)
Glial in origin	60 (64.5%)	Non glial in origin	33 (35.5%)
Intra-axial tumors	82 (88.2%)	Extra-axial tumors	11 (11.8%)

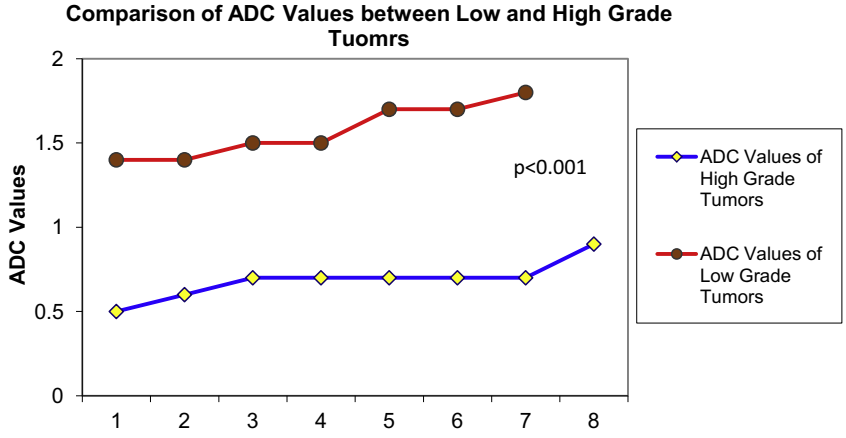

Fig. 1 Comparison of ADC individual values between low and high grade tumors.

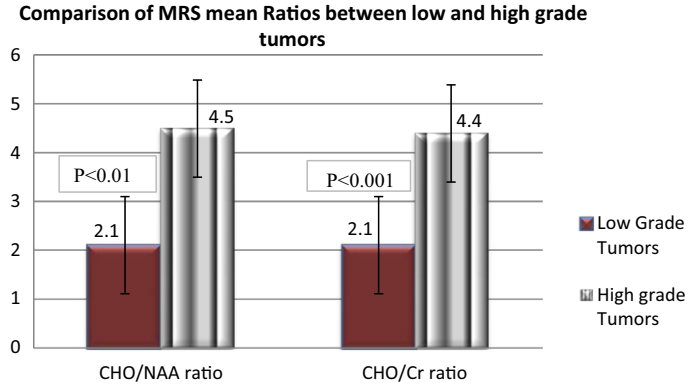

Fig. 2 Bar graph with error bars showing means and confidence intervals of CHO/NAA and CHO/Cr ratios in both low and high grade tumor groups.

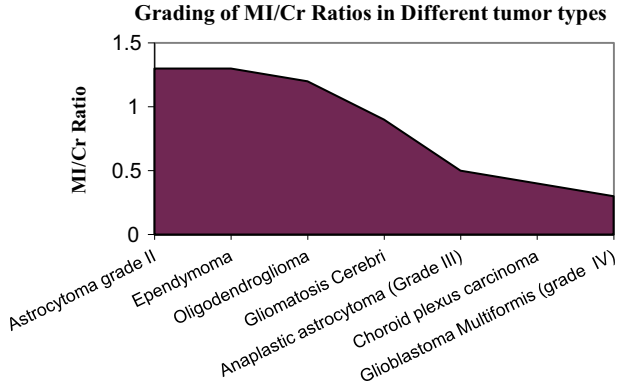

Fig. 3 Showing the grading of mI/Cr ratios from low to high grade tumors.

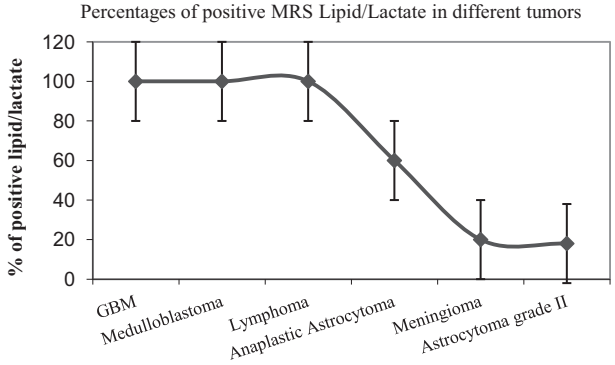

Fig. 4 Showing the percentages of positive MRS lipid/lactate in low and high grade tumors. The tumors represented in the graph are those with more than 2 cases.

metastasis. These cases were diagnosed histopathologically. In addition, MRS has a limited role in brain tumors with massive hemorrhage as massive hemorrhage interferes with spectroscopy results. Finally, in the present study we excluded 52 cases of non neoplastic tumor like conditions. Clinical presentation, combined MRI/MRS, and therapeutic response of these cases were concordant to be non neoplastic. Most of these cases were radiation necrosis, brain infarction, tumefactive MS, brain abscess and brain gliosis (Figs. 9 and 10).

4. Discussion

During the proposal of this study, it was clear to us that MRS alone may have inadequate specificity in diagnosing of

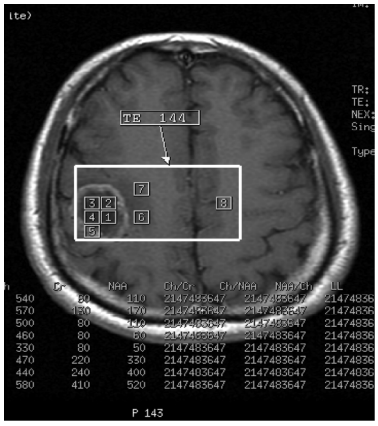

A: MRS voxels (TE 144)

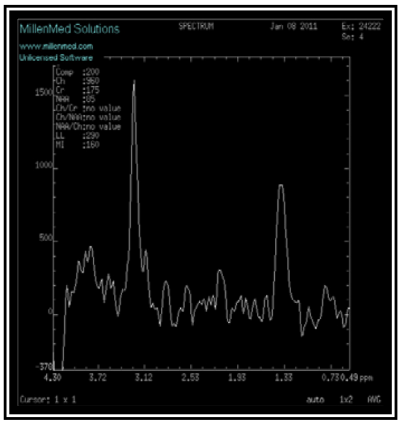

B: Intralesional voxel (TE 144)

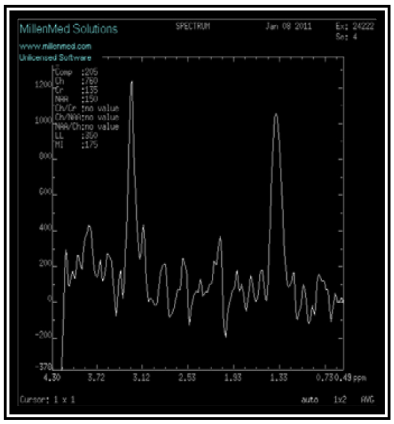

C: Perilesional voxel (TE 144)

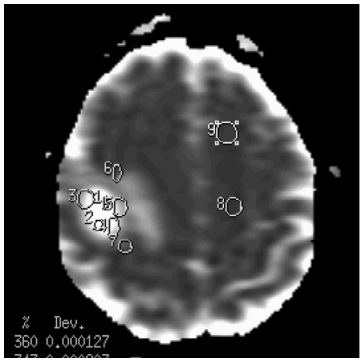

D: ADC map

Fig. 5 Glioblastoma multiformis, male patient, 61 years presented with headache. MRI (A) showed right parietal intraaxial lesion surrounded by grade II vasogenic edema with marginal enhancement of non uniform thickness after IV contrast. DWI shows restricted diffusion with central area of free diffusion, calculated ADC value = 0.5×10^{-3} mm^2 s. MRS: Intra-lesional and perilesional voxels (B, C) shows marked ↑ CHO, marked ↓ of Cr and NAA,with ratios of CHO/NAA = 6.2, CHO/Cr = 5.8, ↑ lipid/lactate also are seen.

Table 2 Role of MRS/ADC in differentiation between specific tumor types.

Tumor type	Mean ADC value	Mean CHO/NAA	Mean CHO/Cr	L/L	Myoinstol	Taurine
1- Medulloblastoma	–	5 .3	5 .2	+ve	absent	+ve
2- Ependymoma	–	2.2	2.3	−ve	elevated	−ve
Tumor type	Mean ADC value	Mean CHO/NAA	Mean CHO/Cr	Mean L/L	–	–
1- Glioblastoma multiformis	0.8	5.6	5.7	+ve	–	–
2- Lymphoma	0.55	3.5	4.5	+ve	–	–
3- Metastasis	–	0.8	0.9		–	–

Table 3 Role of MRS in differentiation between extra-axial brain tumors.

Tumor type	N	CHO	Cr	NAA	L/L	Alanine
1- Meningioma	5	↑	↓	↓	+ve (1) −ve (4)	+ve
2- Acoustic neuroma	1	↑	↓	↓	+ve (1)	+ve
Type of tumor	N	CHO	Cr	NAA	L/L	–
1- Pituitary adenoma	2	↑	↓	↓	−ve	–
2- Craniopharyngioma	1	Absent	Absent	Absent	+ve High	–

different brain lesions despite being highly specific in certain conditions. As well it is unusual in clinical practice that MRS is requested alone, but rather requested with or after MRI as a complementary tool when diagnosis is still doubtful. Therefore the present study was designed to outline the possible diagnostic role of combined MRI/MRS in classification and management of different types of brain tumors. Most of the brain tumors in the present study were glial in origin (64.5%). Shih et al. (10) mentioned that the glial cell tumors are the most common primary central nervous system neoplasm. In agreement with Doolittle (11), the most common glial tumor in our study was GBM (53.3% of all glial tumors).

Diffusion WI was used as indicator of tumor grade by providing information about tumor cellularity. In the present work, there was statistically significant difference between mean calculated ADC values of low and high grade tumors with no significant difference tumor of the same grade. Subsequently, the mean calculated ADC values were considerably effective in grading of malignant tumors. Bulakbasi et al. (12) and Vincentelli et al. (13) agreed with our findings and explained that the greater the density of structures hindering water mobility, the lower the ADC and that the differentiation of pathologic subtypes having the same grade by ADC value is more problematic than grading ratios. Moreover, ADC value could characterize lymphoma from GBM. The ADC value of lymphoma ($0.54 \pm 0.18 \times 10^{-33}$ mm^2 s) was lower than that of GBM ($0.9 \pm 0.047 \times 10^{-33}$ mm^2 s). This can be explained by higher cellularity of lymphoma than GBM (due to presence of necrosis). This is in agreement with Toh et al. (14) who mentioned that the ADC is useful in the distinction between lymphoma and GBM infiltrating the corpus callosum. In addition, combination of DWI and ADC value could differentiate between GBM and metastatic tumors by the presence of tumor infiltration in GBM and perilesional vasogenic edema in metastasis. Lee et al. (15) and Pavlisa et al. (16) agreed with this outcome and verified that DWI showed free diffusion in edema contrary to restriction diffusion in areas of densely packed tumor cells. ADC value is low in tumoral infiltration

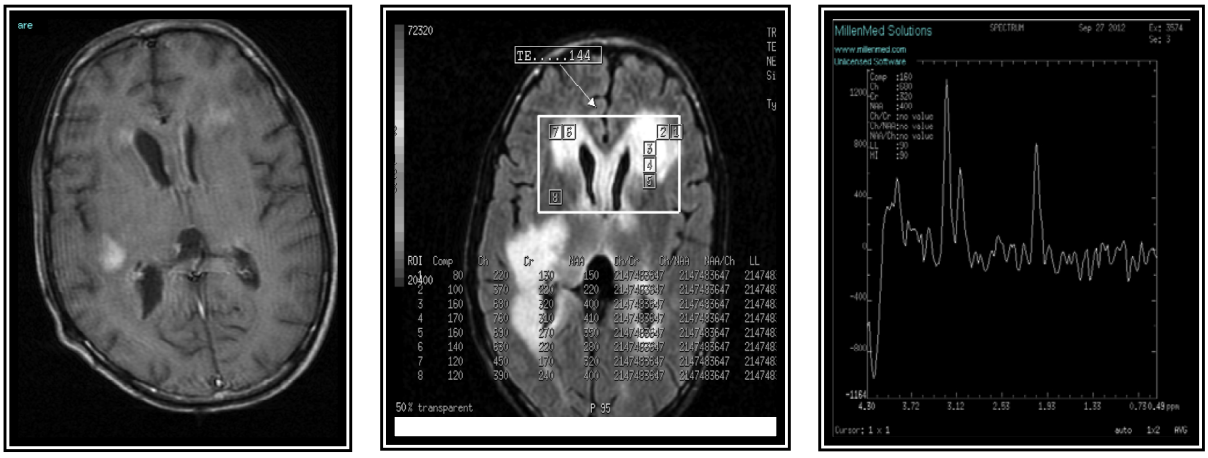

A: Axial T1 (post contrast) B: MRS voxels (TE 144) C: Intralesional (TE 144)

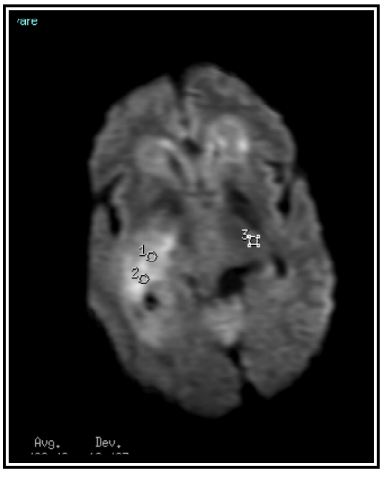

D: ADC map

Fig. 6 Lymphoma; male patient aged 68 years, contrast MRI (A) shows multiple well defined periventricular and deep white matter lesion intra axial SOL in right parietal and bilateral frontal regions, with moderate homogenous enhancement after IV contrast, diffusion WI shows restricted diffusion with calculated ADC value (D) = 0.4×10^{-3} mm^2 s. MRS of intra-lesional voxel (B, C) shows elevation of CHO, reduction of Cr and NAA,with ratios of CHO/NAA = 5.2, CHO/Cr = 5.1 short TE shows moderate elevation of lipid/lactate.

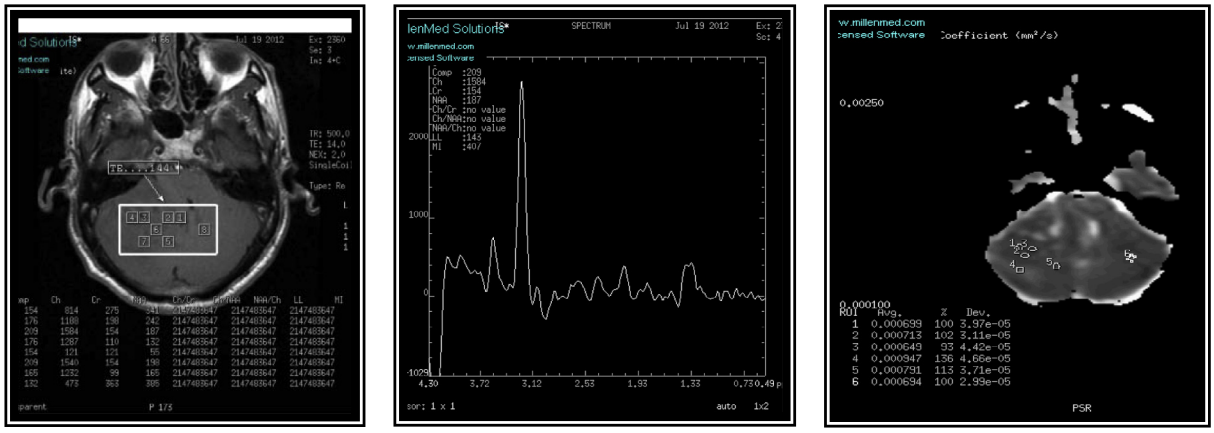

A: MRS voxels (TE 144) B: Intralesional voxel (TE 35) C: ADC map

Fig. 7 Medulloblastoma; male, 20 yrs, presented with headache and ataxia. MRI (A) shows right cerebellar intra axial SOL displaying hypo intense signal in T1 WI, with mild enhancement after IV contrast, .The lesion is surrounded by mild vasogenic edema. DWI shows restricted diffusion, ADC value = 0.6×10^{-3} mm^2 s. MRS intra-lesional voxel shows marked ↑ CHO, marked ↓ Cr and NAA, CHO/NAA = 6.5, CHO/Cr = 6.2, with ↑ of lipid/lactate. Taurine is present at 3.4 ppm (B).

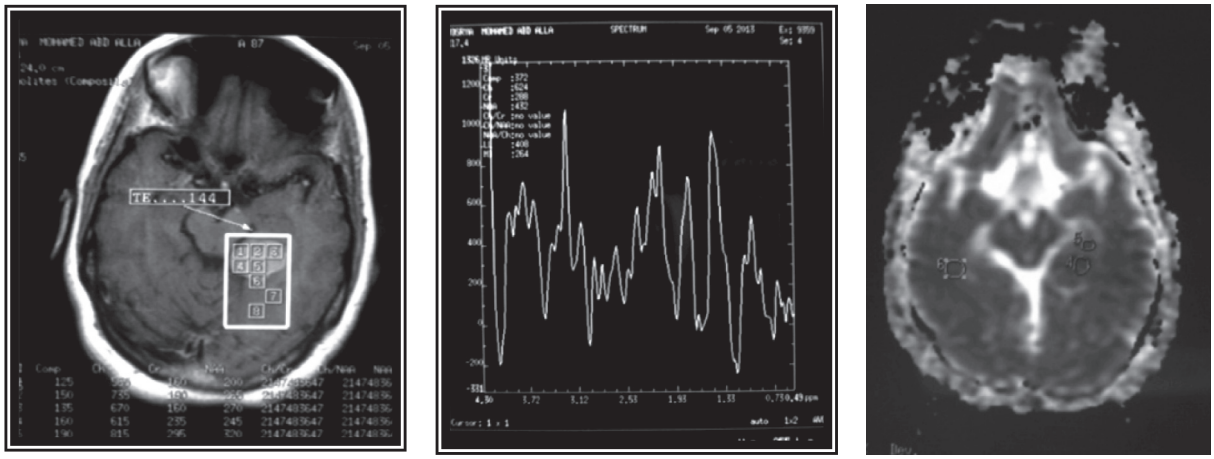

A: MRS voxels (TE 144) B: Intralesional voxel (TE 35) C: ADC map

Fig. 8 Meningioma; female, 40 years presented with epilepsy. MRI (A) shows left temporal extra axial SOL displaying iso-intense signal in T1 with marked homogenous enhancement after IV contrast, no restricted diffusion could be detected, calculated ADC value (C) = 1.7×10^{-3} mm^2 s. MRS shows mild ↑ of CHO, with mild ↓ of NAA and Cr, CHO/NAA = 1.9, CHO/Cr = 1.8. Short TE shows ↑ level of alanine (B), (specific for meningioma), with mild ↑ of lipid/lactate.

and high in peritumoral edema. Further, in concordant with Yamasaki et al. (4), the ADC value of craniopharyngioma (1.9×10^{-33} mm^2 s) was higher than that of pituitary adenoma ($1.7 \pm 0.2 \times 10^{-33}$ mm^2 s).

In the present study we used MVS as it has the ability to survey the whole neoplastic area, peritumoral area for infiltration and edema. Both long and short TE (144 and 35 ms) were used. The spectra of long TE can easily detect and quantify peaks of NAA, CHO and Cr (17). In general, MRS of intracranial neoplasms typically shows elevated choline and reduced NAA and creatine. McKnight et al. (18) have shown that the Choline/NAA and Choline/Cr ratios are in parallel with cell density, proliferative index and the ratio of proliferation to cell death. As well, both ratios increase with an increase in grade of malignancy. In our cohort of patients, the significance of CHO/NAA and CHO/Cr ratios in diagnosis and grading of brain tumor has been demonstrated. CHO/Cr ratio was more significant ($P < 0.001$) than CHO/NAA ratio ($P < 0.01$). Further, GBM had higher CHO/NAA and CHO/Cr ratios than anaplastic astrocytoma. Brandao et al. (19) similarly reported a statistically significant higher Cho/Cr, Cho/NAA in high grade gliomas and added that Cho/Cr ratio is specifically useful in grading of brain gliomas. By contrast, Howe et al. (20) stated that Cho/Cr is elevated in grade III more than Grade IV gliomas because of prominent necrosis that is usually present in grade IV gliomas. This disagreement may be explained by that we intentionally choose and placed the voxels in the most enhanced solid parts away from necrotic areas. Additional importance of MRS parameters in discrimination of brain neoplasms was found. MRS could distinguish between GBM and metastasis by calculating perilesional CHO/NAA and CHO/Cr ratios. GBM showed high CHO/NAA and

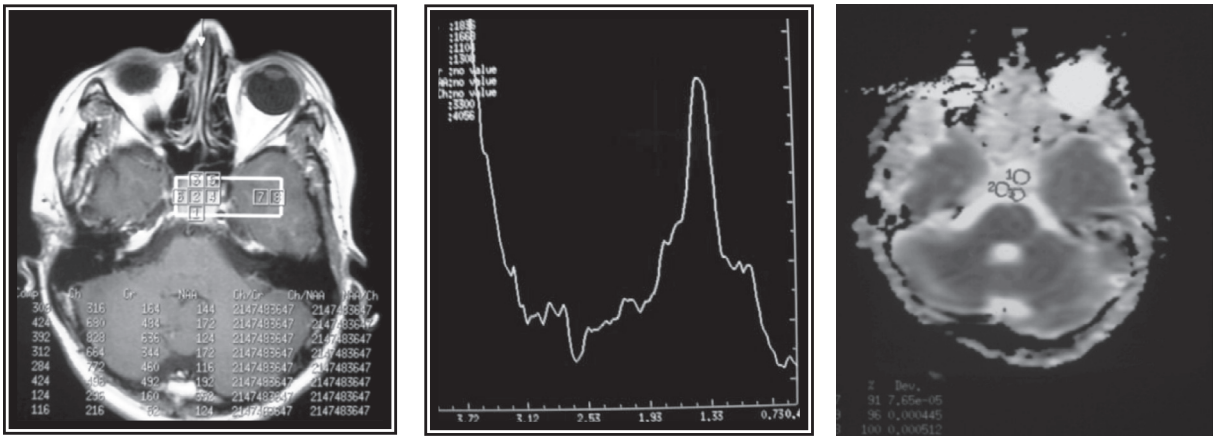

A: MRS voxels (TE 144) B: Intralesional voxel (TE 35) C: ADC map

Fig. 9 Craniopharyngioma; male, 19 years presented with visual impairment. MRI (A) shows sellar and suprasellar lesion with mixed cystic and solid component with mild homogenous enhancement of the solid part after IV contrast, no restricted diffusion could be detected. ADC value (C) = 1.9×10^{-33} mm^2 s. MRS (B) shows marked ↑ of lipid/lactate with absent other metabolites.

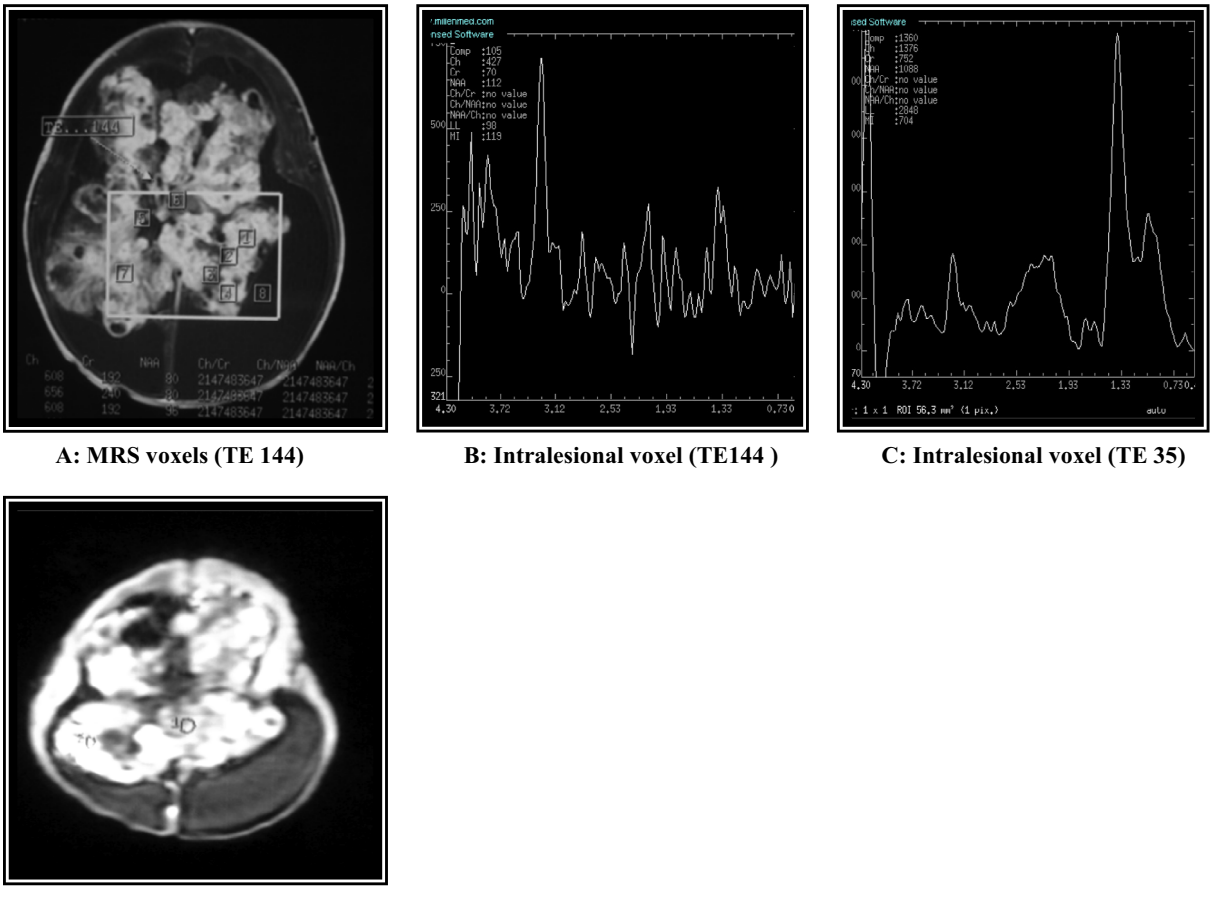

A: MRS voxels (TE 144) B: Intralesional voxel (TE144) C: Intralesional voxel (TE 35)

D: ADC map

Fig. 10 Choroid plexus carcinoma; one month old infant presented with a large head. MRI (A) shows Intra ventricular SOL occupying the lateral ventricle with marked homogenous enhancement after IV contrast. Diffusion WI shows restricted diffusion with calculated ADC value (D) = 0.7×10^{-3} mm^2 s. MRS intra-lesional voxel (B, C) shows marked elevation of CHO, marked reduction of Cr and NAA,with ratios of CHO/NAA = 4.4, CHO/Cr = 3.8 short TE shows marked elevation of lipid/lactate.

CHO/Cr ratios denoting tumor infiltration while metastasis showed normal CHO/NAA and CHO/Cr ratios denoting peri-lesional vasogenic edema. Brandao et al. (19) declared comparable conclusions. Similar to findings of Castillo et al.

(21) and Howe et al. (20), the mI/Cr ratios showed an inverse relationship with tumor grade (higher in patients with low-grade astrocytoma, ependymoma, oligodendroglioma and lower in patients with anaplastic astrocytoma, choroid plexus carcinoma and GBM). Myoinositol is a glial marker because it is primarily synthesized in glial cells, almost only in astrocytes. The presence of lactate and lipids denotes high grade tumors. With increasing malignancy, tumors showed increasing lactate and lipid peaks with significant difference for lipid and lactate between low and high grade tumors. Bulik et al. (22) accomplished a similar result. According to Shih et al. (10), the peak of lactate is barely seen in normal brain. Lactic acid is a product of anaerobic glycolysis so its concentration increases under anaerobic metabolism in malignant tumors. Van der Graaf (23) added that lipid peak can be seen when there is cellular membrane breakdown or necrosis such as in metastases or primary malignant tumors. In agreement with Vuori et al. (24), the spectroscopic findings of the present work could differentiate between astrocytoma grade II and oligodendroglioma. Oligodendroglioma showed prominent elevation of CHO and Cr, while grade II astrocytoma showed a mild increase in CHO and a decrease in Cr. Furthermore, MVS has a significant role in differentiation between craniopharyngioma and pituitary adenoma. Pituitary adenoma was seen in two cases, that showed prominent CHO peak with low levels of NAA and creatine while craniopharyngioma showed absent CHO, NAA, Cr with dominant lipid/lactate peak (high cholesterol content). Faghih et al. (25) have shown analogous findings. On the other hand, quite different results have been reported by Sutton et al. (26) They stated that all the pituitary adenomas showed prominent peak of choline with no other metabolites. The presence of NAA and Cr with dominant CHO peak in our results may be explained by contamination with neural tissue. For the 5 cases of meningioma, MRS showed unique presence of alanine in addition to increased choline, reduced creatine and NAA. This is in accordance with other authors (23,27) who declared that the most characteristic feature of meningiomas is the presence of alanine. One case of acoustic neuronal was included in our study. MRS showed a similar spectroscopic picture to that of meningioma cases. However, there was elevated lipid and lactate which may be related to the presence of cystic component of the tumor. Brandao et al. (19) explained that lipids do not necessarily represent necrosis but may be related to the presence of cysts. MRS was insignificant in differentiating between meningioma and acoustic neuroma due to similar spectroscopic picture of both tumors. The MRS of 3 cases of cerebellar medulloblastoma characteristically showed the presence of taurine which is the most specific metabolite for diagnosis of medulloblastoma in addition to elevated Cho/Cr and Cho/NAA ratios, and presence of lipid and lactate. Spectroscopy was significant in differentiation between medulloblastoma and ependymoma. Medulloblastoma cases showed a marked presence of taurine, lipid and lactate which are absent in epenymoma. As well, there were higher CHO/NAA and CHO/Cr ratios in medulloblastoma cases than in ependymoma cases. On the other hand myo instol is elevated in ependymoma and absent in medulloblastoma. This is in accordance with Majos et al. (28) who verified that the elevation of the Cho peak, Cho/Cr and Cho/NAA ratios in medulloblastomas is linked to the high cell density and reflecting its malignant nature.

Comparative results of combined MRI/MRS and histopathological established that the diagnostic accuracy of combined MRI/MRS was 91%, with high sensitivity (91%) and specificity (90.5%). Comparable findings were mentioned by other investigators (29,30). Majós et al. (31) also elucidated that brain tumor classification using spectroscopy was accurate in 105 of 112 cases, with an accuracy of 94%. Expectedly, eight out of 93 cases were mis-graded or mis-diagnosed by MRS. The spectroscopic overlapping is well known and has been documented by many authors. Brandao et al. (19) showed some overlap between grades II and III astrocytomas also between GBM and metastasis. The overlap between GBM and metastasis was explained that the high MRS parameters in the peritumoral region surrounding a GBM may not be demonstrated in the spectrum, as these changes are related to a number of tumor cells that have infiltrated the peritumoral area. If no elevation of the CHO peak is seen in the peritumoral area, a high grade primary tumor cannot be ruled out. Although not directly tested, MRS potentially plays an important role in biopsy guidance to recognize regions of high metabolic activity. This is especially important when histopathology is not helpful due to sampling errors or only a few small tissue samples were obtained by stereotactic biopsy. Chernov et al. (32) revealed that compared to MRI-guided technique they have described an increase in the diagnostic yields of MRS-supported stereotactic brain biopsies from 90% to 100%. Finally, this study showed that MRS had a valuable role in differentiation between tumor recurrence and radiation necrosis. Smith et al. (33) demonstrated that the distinction between recurrent tumor and radiation necrosis using the Cho/NAA ratio could be made with 85%sensitivity and 69% specificity.

In conclusion, combined calculated ADC values from DWI and MRS techniques, have yielded a significant synergetic potency in diagnosis of intracranial neoplasms. MRS has robust diagnostic accuracy in cases of well defined high or low grad brain neoplasms. ADC value had the ability to confirm and differentiate low from high grade tumors in many situations where there were diagnostic confusions with MRS due to borderline values. To a significant extent, our inferences can be reflected on clinical practice and decision making, as it may obviate or at least minimize the need for more invasive diagnostic techniques. Other potential benefits include, measuring treatment effect, guidance of brain biopsy, differentiation between radiation necrosis and tumor recurrence, follow up of brain tumors and differentiation between neoplastic and non neoplastic tumor like conditions.

Authors contributions

A. El Sherbini, M. El Shafie and M. Hefeda, contributed to study design and interpretation. A. El Shebini has contributed to all MRS/MRI procedures. A. Seiam contributed to data analysis and interpretation. All biopsies were taken by A. Shakal. S. Biomy has done histopathology for all cases. A. El Sherbini, M. Hefeda and A. Seiam contributed to article preparation.

Ethics approval

This protocol was approved by the Research Ethics committee of the Tanta Medical School, Tanta, Egypt.

Conflict of interest

We have no conflict of interest to declare.

References

(1) Vicente J, Fuster-Garcia E, Tortajada S, et al. Accurate classification of childhood brain tumours by in vivo 1H. Eur J Cancer 2013;49:658–67.
(2) Young GS. Advanced MRI of adult brain tumors. Neurol Clin 2007;25(viii):947–73.
(3) Provenzale JM, Mukundan S, Barboriak DP. Diffusion-weighted and perfusion MR imaging for brain tumor characterization and assessment of treatment response. Radiology 2006;239:632–49.
(4) Yamasaki F, Kurisu K, Satoh K, et al. Apparent diffusion coefficient of human brain tumors at MR imaging. Radiology 2005;235:985–91.
(5) Sibtain NA, Howe FA, Saunders DE. The clinical value of proton magnetic resonance spectroscopy in adult brain tumours. Clin Radiol 2007;62:109–19.
(6) Orphanidou-Vlachou E, Auer D, Brundler MA, et al. (1)H magnetic resonance spectroscopy in the diagnosis of paediatric low grade brain tumours. Eur J Radiol 2013;82:295–301.
(7) Lamiaa IA, Sally E, Omar A, Iman MH, Amr KE, Ahmed MA. Predicting grade of cerebral gliomas using Myoinositol/Creatine ratio. Egypt J Radiol Nucl Med 2014;45:211–7.
(8) Dowling C, Bollen AW, Noworolski SM, et al. Preoperative proton MR spectroscopic imaging of brain tumors: correlation with histopathologic analysis of resection specimens. AJNR Am J Neuroradiol 2001;22:604–12.
(9) Louis DN, Ohgaki H, Wiestler OD, et al. The 2007 WHO classification of tumours of the central nervous system. Acta Neuropathol 2007;114:97–109.
(10) Shih MT, Singh AK, Wang AM, Patel S. Brain lesions with elevated lactic acid peaks on magnetic resonance spectroscopy. Curr Probl Diagn Radiol 2004;33:85–95.
(11) Doolittle ND. State of the science in brain tumor classification. Semin Oncol Nurs 2004;20:224–30.
(12) Bulakbasi N, Guvenc I, Onguru O, Erdogan E, Tayfun C, Ucoz T. The added value of the apparent diffusion coefficient calculation to magnetic resonance imaging in the differentiation and grading of malignant brain tumors. J Comput Assist Tomogr 2004;28:735–46.
(13) Vincentelli C, Hwang SN, Holder CA, Brat DJ. The use of neuroimaging to guide the histologic diagnosis of central nervous system lesions. Adv Anat Pathol 2012;19:97–107.
(14) Toh CH, Castillo M, Wong AM, et al. Primary cerebral lymphoma and glioblastoma multiforme: differences in diffusion characteristics evaluated with diffusion tensor imaging. AJNR Am J Neuroradiol 2008;29:471–5.
(15) Lee EJ, terBrugge K, Mikulis D, et al. Diagnostic value of peritumoral minimum apparent diffusion coefficient for differentiation of glioblastoma multiforme from solitary metastatic lesions. AJR Am J Roentgenol 2011;196:71–6.
(16) Pavlisa G, Rados M, Pavlisa G, Pavic L, Potocki K, Mayer D. The differences of water diffusion between brain tissue infiltrated by tumor and peritumoral vasogenic edema. Clin Imaging 2009;33:96–101.
(17) Lukas L, Devos A, Suykens JA, et al. Brain tumor classification based on long echo proton MRS signals. Artif Intell Med 2004;31:73–89.
(18) McKnight TR, Lamborn KR, Love TD, et al. Correlation of magnetic resonance spectroscopic and growth characteristics within Grades II and III gliomas. J Neurosurg 2007;106:660–6.
(19) Brandao LA, Shiroishi MS, Law M. Brain tumors: a multimodality approach with diffusion-weighted imaging, diffusion tensor imaging, magnetic resonance spectroscopy, dynamic susceptibility contrast and dynamic contrast-enhanced magnetic resonance imaging. Magn Reson Imaging Clin N Am 2013;21:199–239.
(20) Howe FA, Barton SJ, Cudlip SA, et al. Metabolic profiles of human brain tumors using quantitative in vivo 1H magnetic resonance spectroscopy. Magn Reson Med 2003;49:223–32.
(21) Castillo M, Smith JK, Kwock L. Correlation of myo-inositol levels and grading of cerebral astrocytomas. AJNR Am J Neuroradiol 2000;21:1645–9.
(22) Bulik M, Jancalek R, Vanicek J, Skoch A, Mechl M. Potential of MR spectroscopy for assessment of glioma grading. Clin Neurol Neurosurg 2013;115:146–53.
(23) van der Gaaf G. In vivo magnetic resonance spectroscopy: basic methodology and clinical applications. Eur Biophys J 2010;39:527–40.
(24) Vuori K, Kankaanranta L, Hakkinen AM, et al. Low-grade gliomas and focal cortical developmental malformations: differentiation with proton MR spectroscopy. Radiology 2004;230:703–8.
(25) Faghih JM, Ghodsi SM, Akhlaghpoor S, et al. Complementary effect of H MRS in diagnosis of suprasellar tumors. Clin Imaging 2012;36:810–5.
(26) Sutton LN, Wang ZJ, Wehrli SL, et al. Proton spectroscopy of suprasellar tumors in pediatric patients. Neurosurgery 1997;41:388–94.
(27) Demir MK, Iplikcioglu AC, Dincer A, Arslan M, Sav A. Single voxel proton MR spectroscopy findings of typical and atypical intracranial meningiomas. Eur J Radiol 2006;60:48–55.
(28) Majos C, Alonso J, Aguilera C, et al. Adult primitive neuroectodermal tumor: proton MR spectroscopic findings with possible application for differential diagnosis. Radiology 2002;225:556–66.
(29) Preul MC, Caramanos Z, Collins DL, et al. Accurate, noninvasive diagnosis of human brain tumors by using proton magnetic resonance spectroscopy. Nat Med 1996;2:323–5.
(30) Hollingworth W, Medina LS, Lenkinski RE, et al. A systematic literature review of magnetic resonance spectroscopy for the characterization of brain tumors. AJNR Am J Neuroradiol 2006;27:1404–11.
(31) Majos C, Julia-Sape M, Alonso J, et al. Brain tumor classification by proton MR spectroscopy: comparison of diagnostic accuracy at short and long TE. AJNR Am J Neuroradiol 2004;25:1696–704.
(32) Chernov MF, Muragaki Y, Ochiai T, et al. Spectroscopy-supported frame-based image-guided stereotactic biopsy of parenchymal brain lesions: comparative evaluation of diagnostic yield and diagnostic accuracy. Clin Neurol Neurosurg 2009;111:527–35.
(33) Smith EA, Carlos RC, Junck LR, Tsien CI, Elias A, Sundgren PC. Developing a clinical decision model: MR spectroscopy to differentiate between recurrent tumor and radiation change in patients with new contrast-enhancing lesions. AJR Am J Roentgenol 2009;192:45–52.